

The Coffee-table Book of Pseudospectra

Vincent Heuveline
Chandramowli Subramanian

No. 2012-03

Preprint Series of the Engineering Mathematics and Computing Lab (EMCL)





Preprint Series of the Engineering Mathematics and Computing Lab (EMCL)
ISSN 2191-0693
No. 2012-03

Impressum

Karlsruhe Institute of Technology (KIT)
Engineering Mathematics and Computing Lab (EMCL)

Fritz-Erler-Str. 23, building 01.86
76133 Karlsruhe
Germany

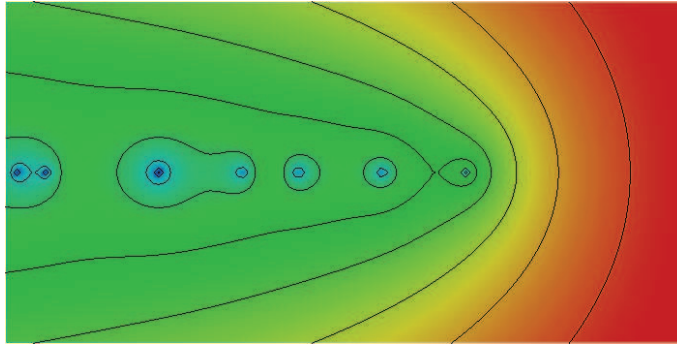
KIT – University of the State of Baden Wuerttemberg and
National Laboratory of the Helmholtz Association

Published on the Internet under the following Creative Commons License:
<http://creativecommons.org/licenses/by-nc-nd/3.0/de> .



www.emcl.kit.edu

THE
COFFEE-TABLE BOOK
OF
PSEUDOSPECTRA



VINCENT HEUVELINE, CHANDRAMOWLI SUBRAMANIAN
Engineering Mathematics and Computing Lab
Karlsruhe Institute of Technology

1 Introduction

The key issue of hydrodynamic stability is the investigation of spectral properties of the underlying system describing the fluid flow. Since in many applications the governing operators are strongly nonnormal, an analysis based on eigenvalues only may be misleading. As a remedy, pseudospectra have become a popular tool to investigate spectral properties, where a traditional eigenvalue analysis fails. Pseudospectra provide more information about the behavior of a system as they constitute a more general tool than eigenvalues.

The intention of this manuscript is to present pseudospectra of fluid flow problems rather than to give an extensive discussion on all the involved backgrounds. The evaluation is done by exploiting parallel computational techniques which allows us to address complex problems. In the following Sections we give a short review of hydrodynamic stability and the role of pseudospectra in this context. Afterwards we present extensive numerical results, i.e. spectral portraits of different fluid flow problems with different setups.

2 Hydrodynamic Stability

The approach of hydrodynamic stability is to investigate how a laminar fluid flow behaves with respect to perturbations. If the perturbation decays in time and the flow returns to its original state it is said to be stable. On the other hand, if the perturbation causes the flow to change into a different state, it is said to be unstable. Instability may trigger turbulence, but it may also take the flow to a different laminar state.

There are two main approaches for the study of hydrodynamic stability. The *nonlinear stability* theory is based on examining the kinetic energy of the flow by means of integral inequality techniques. The *linear stability* theory is concerned with a linearized model of the fluid flow and establishes statements by means of the spectrum of the linearized operator. If all eigenvalues lie in the left half of the complex plane, the flow is said to be linear stable. If there is at least one eigenvalue in the right half of the complex plane, the flow is linear unstable.

We consider a viscous fluid flow with velocity \mathbf{v} and pressure p governed by the incompressible Navier-Stokes equations

$$\begin{aligned} -\nu\Delta\mathbf{v} + (\mathbf{v} \cdot \nabla)\mathbf{v} + \nabla p &= \mathbf{0}, \\ \nabla \cdot \mathbf{v} &= 0 \end{aligned} \tag{1}$$

in a bounded domain Ω . For simplicity we have set $\rho = 1$. Furthermore, ν denotes the kinematic viscosity and \mathbf{f} some prescribed external force. We assume the boundary $\Gamma = \partial\Omega$ to be disjointly comprised of $\Gamma = \Gamma_{rigid} \cup \Gamma_{in} \cup \Gamma_{out}$. As an inflow condition we set

$$\mathbf{v} = \mathbf{v}_{in} \quad \text{on } \Gamma_{in}$$

with a given function \mathbf{v}_{in} . On Γ_{rigid} we impose *no-slip* boundary conditions, i.e.

$$\mathbf{v} = \mathbf{0} \quad \text{on } \Gamma_{rigid}.$$

Furthermore, we prescribe free-stream outflow conditions (or *do-nothing* conditions)

$$\nu\partial_{\mathbf{n}}\mathbf{v} - p\mathbf{n} = 0 \quad \text{on } \Gamma_{out},$$

where \mathbf{n} refers to the outward unit normal.

Assume a steady solution (\mathbf{V}, P) which stability we want to investigate is known (either numerically or even analytically). The linear stability problem is formulated by means of an eigenvalue problem which is derived by a linearization around (\mathbf{V}, P) seeking for the eigenvalues λ and the eigenmodes $(\tilde{\mathbf{v}}, \tilde{p})$ of

$$\begin{aligned}\lambda\tilde{\mathbf{v}} &= \nu\Delta\tilde{\mathbf{v}} - (\tilde{\mathbf{v}} \cdot \nabla)\mathbf{V} - (\mathbf{V} \cdot \nabla)\tilde{\mathbf{v}} - \nabla\tilde{p}, \\ 0 &= \nabla \cdot \tilde{\mathbf{v}}\end{aligned}\tag{2}$$

in Ω , see e.g. [9, 10]. The boundary conditions are prescribed by

$$\tilde{\mathbf{v}}|_{\Gamma_{rigid}} = \mathbf{0}, \quad \tilde{\mathbf{v}}|_{\Gamma_{in}} = \mathbf{0}, \quad \nu\partial_{\mathbf{n}}\tilde{\mathbf{v}} - \tilde{p}\mathbf{n}|_{\Gamma_{out}} = 0.$$

All eigenvalues λ of (2) are either real or occur in complex conjugate pairs. If $\text{Re } \lambda < 0$, the corresponding mode dies out in time. Whereas a mode with $\text{Re } \lambda > 0$ results in instability. Finally, a mode with $\text{Re } \lambda = 0$ is called neutrally stable and may trigger nonlinear instability.

Assume we have countably many eigenvalues with no accumulation point at 0. Then, we have that the basic flow of the linearized problem is stable with respect to a perturbation consisting of a superposition of eigenmodes if all normal modes are stable, i.e. $\text{Re } \lambda < 0$ for all eigenvalues (see [9, 10]). If there exists at least one eigenvalue λ with $\text{Re } \lambda > 0$, the basic flow is instable.

The *Reynolds number* is crucial for the stability behavior and is defined by $Re = VL/\nu$ with characteristic velocity V and characteristic length L . Typically, a flow becomes instable as the Reynolds passes a certain threshold, which is called *critical Reynolds number*. Hence, the critical Reynolds number Re_c is defined as the smallest number such that the basic flow under consideration is stable for all $Re \leq Re_c$, and becomes instable for a $Re > Re_c$.

Note that linear stability does not guarantee stability in general, whereas linear instability means also instability. Hence, the linear stability theory can provide us an upper bound for Re_c if for any $Re > Re_c$ at least one eigenvalue of (2) has a positive real part. In order to determine also a lower bound one could employ nonlinear techniques. However, in this work we consider pseudospectra as an approach to track down the critical Reynolds number as, even for simple setups, a traditional linear stability analysis by means of the spectrum only may not reveal instability which is experienced in laboratory experiments (see [18] and references therein). For example, let us consider a dynamical system describing the evolution of a perturbation u by

$$\frac{d}{dt}u = Au$$

with a linear operator A . Under certain conditions the solution can be expressed in forms of an operator exponential $e^{tA}u_0$, where u_0 represents the initial disturbance $u(0)$. If the spectrum of A lies in the left half of the complex plane, $e^{tA}u_0$ tends to zero as $t \rightarrow \infty$ and no instability is detected. Nevertheless, $e^{tA}u_0$ may become arbitrarily large for finite t , which can trigger instabilities.

3 Pseudospectra

In the sequel, let $(X, \|\cdot\|)$ be a Banach space and $A : X \rightarrow X$ a bounded linear operator. The spectrum of A is denoted by $\sigma(A)$. We write $z - A$ instead of $zI - A$, where I denotes

the identity on X . For $z \notin \sigma(A)$ we have the inequality $\|(z - A)^{-1}\| \geq (\text{dist}(z, \sigma(A)))^{-1}$. Therefore, we set as convention $\|(z - A)^{-1}\| = \infty$ if $z \in \sigma(A)$. Then, for any $\varepsilon > 0$ the ε -pseudospectrum of A is equivalently defined by

$$\sigma_\varepsilon(A) = \{z \in \mathbb{C} : \|(z - A)^{-1}\| > \varepsilon^{-1}\}, \quad (3)$$

$$= \{z \in \mathbb{C} : z \in \sigma(A + \Delta A) \text{ for some bounded operator } \Delta A \text{ with } \|\Delta A\| < \varepsilon\}, \quad (4)$$

$$= \{z \in \mathbb{C} : \|(z - A)u\| < \varepsilon \text{ for some } u \in X \text{ with } \|u\| = 1\}, \quad (5)$$

see [17].

A lower bound for $\|e^{tA}\|$ reflecting that the spectrum gives sufficient information about instability is given by

$$\|e^{tA}\| \geq e^{t\alpha(A)}, \quad (6)$$

where the spectral abscissa is defined as usual by $\alpha(A) = \sup_{z \in \sigma(A)} \text{Re } z$. However, the information retrieved by the spectrum of A does not tell the full story. As we will show in the following Theorem, if the spectrum lies in the left half-plane and the pseudospectrum of A protrudes significantly into the right half-plane, there is a transient growth which is not indicated by (6). Here, let $\alpha_\varepsilon(A) = \sup_{z \in \sigma_\varepsilon(A)} \text{Re } z$ denote the ε -pseudospectral abscissa.

Theorem 3.1 *Defining the Kreiss constant by*

$$\mathcal{K}(A) = \sup_{\varepsilon \geq 0} \frac{\alpha_\varepsilon(A)}{\varepsilon} = \sup_{\text{Re } z > 0} (\text{Re } z) \|(z - A)^{-1}\|$$

we have that

$$\sup_{t \geq 0} \|e^{tA}\| \geq \mathcal{K}(A). \quad (7)$$

If $a = \text{Re } z > 0$ and $L = \text{Re } z \|(z - A)^{-1}\|$, then

$$\sup_{0 < t \leq \tau} \|e^{tA}\| \geq e^{\tau a} \left/ \left(1 + \frac{e^{\tau a} - 1}{L} \right) \right. \quad (8)$$

for all $\tau > 0$.

In order to evaluate pseudospectra numerically, we employ finite element methods which are already well established for incompressible fluid flow problems. For elliptic operators there exists a spectral approximation theory [2, 4, 13, 14]. It is based on the results of the spectral approximation theory for compact operators by considering the compact inverse of the operator. Since the evaluation of pseudospectra with respect to the two-norm results in a singular value problem, we apply these results to obtain the same convergence rate as for eigenvalues, namely

$$\mathcal{O}(h^{2(r-m)/\alpha}),$$

see [16]. Here, $r - 1$ is the polynomial degree of the finite element approximation, $2m$ is the order of the elliptic operator, and α is the ascent of the singular value.

Following the definition of pseudospectra, we define the spectral portrait (with respect to the two-norm) of a matrix A by the plot of the map

$$z \mapsto sp_{(A)}(z) = \log_{10} [\|(z - A)^{-1}\|_2] = -\log_{10} [s_{\min}(z - A)], \quad (9)$$

Algorithm 1 Draw spectral portrait of a matrix pencil

```
1: function DRAW_PORTRAIT( $A, (x_1, x_2), (y_1, y_2), nx, ny$ )
2:    $h_x = \frac{x_2 - x_1}{nx - 1}, \quad h_y = \frac{y_2 - y_1}{ny - 1};$ 
3:    $z = x_1 + iy_1;$ 
4:   for  $j = 1, \dots, nx$  do
5:     for  $k = 1, \dots, ny$  do
6:       Compute  $s_{\min}(z - A)$  with the Davidson method;
7:       // Start with the previous computed singular subspace
8:        $z = z + ih_y;$  // Next line
9:     end for
10:     $z = z - ih_y + h_x;$  // Next column
11:     $h_y = -h_y;$  // Change sweep direction along the column
12:  end for
13: end function
```

where $s_{\min}(z - A)$ denotes the smallest singular value of the matrix $z - A$.

For large sparse matrices a complete singular value decomposition induces high computational costs and high storage requirements. Furthermore, we are only interested in the smallest singular value. Since $s_{\min}((z - A)^2) = \lambda_{\min}((z - A)^H(z - A))$, one may apply an efficient sparse symmetric eigenvalue solver on $(z - A)^H(z - A)$. In this context the Davidson method [7, 8] was successfully employed [5, 11, 15].

To draw the spectral portrait of a matrix A in a rectangular domain $[x_1, x_2] \times [y_1, y_2] \subset \mathbb{C}$ we choose a grid of $nx * ny$ points (nx in the horizontal, ny in the vertical) and compute the smallest singular value $s_{\min}(z - A)$ for any z on the grid with the Davidson method. For two neighboring grid points z_1 and z_2 , we expect the matrices $z_1 - A$ and $z_2 - A$ to have close singular values and close singular vectors. Therefore, to improve performance, for a given grid point we start the Davidson algorithm with the singular subspace computed in the last step. The complete solution procedure is outlined in Algorithm 1, see [5, 11].

For different grid points the computation of singular values is completely independent, which allows an easy way to parallelize Algorithm 1. However, this implies that a copy of the needed matrices is available to each process. In order to avoid high storage costs in the case of large matrices, we utilize a parallel linear algebra [1, 12] as well.

This approach is referred to as *hybrid parallelism*. We partition the domain of grid points in \mathbb{C} into k subdomains of the same size. Then p processes are mapped to each of these subdomain of grid points building k groups, provided that we have $k \times p$ processes available. Within each group the system matrices and vectors are spread among the processes in order to perform a parallel computation of the smallest singular vector, see Figure 1.

In the following Sections we present spectral portraits of fluid flow problems, i.e. for given $z \in \mathbb{C}$ we plot $\log_{10}(s_{h,\min}(z))$ where $s_{h,\min}(z)$ is the smallest eigenvalue of

$$(z\mathbf{M}_h - \mathbf{A}_h)^H(z\mathbf{M}_h - \mathbf{A}_h)x_h = s_h^2 \mathbf{M}_h^H \mathbf{M}_h x_h. \quad (10)$$

Here, \mathbf{A}_h denotes the *stiffness matrix* and \mathbf{M}_h the *mass matrix* of the finite element discretization. For details we refer to [16].

For each benchmark we listed the essential parameters:

- The integer n denotes the number of unknowns resulting from the finite element

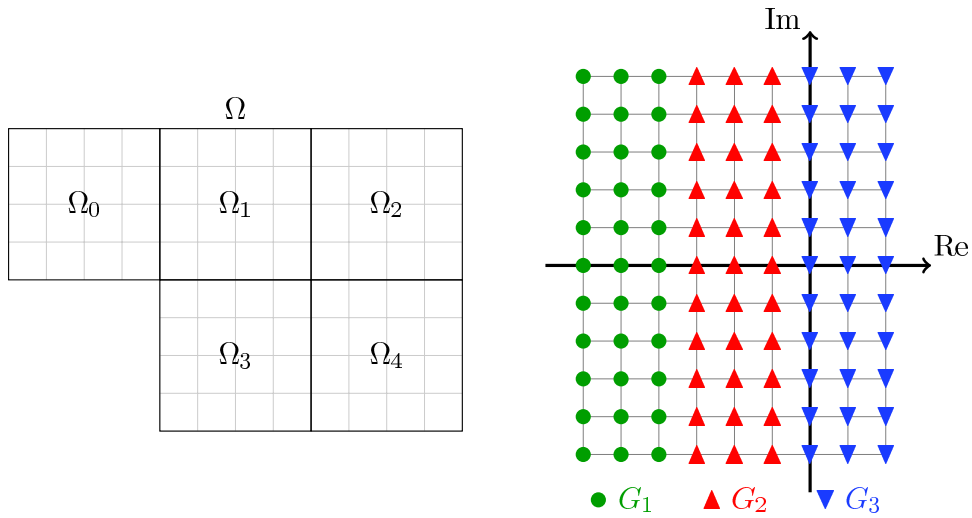


Figure 1: The left figure shows a decomposition of the domain Ω which is used to perform parallel linear algebra operations. The right figure depicts the distribution of grid points in $[x_1, x_2] \times [y_1, y_2] \subset \mathbb{C}$.

approximation scheme chosen.

- The region in the complex domain where the spectral portraits are plotted.
- The grid in the complex domain and the resulting number of computed singular values. Please note that the spectral portraits considered here are symmetric along the real axis.
- The plotted contour lines of the spectral portraits, i.e. the pseudospectra.
- The Reynolds number $Re = VL/\nu$ with characteristic velocity V , characteristic length L , and kinematic viscosity ν .

4 Numerical Results

4.1 Lid-driven Cavity

The investigation of viscous flow in rectangular cavities is of great theoretical importance. But it is also widely used to benchmark numerical methods approximating incompressible fluid flows, see [3] and references therein. In this setup we consider the two-dimensional case with the fluid confined in an unit cube with rigid boundaries at the left, at the right, and at the bottom. The top lid moves uniformly resulting in the inflow condition $\mathbf{v}_{in} = (1, 0)^T$ at the upper boundary Γ_{in} .

- $n = 148,739$
- Region in \mathbb{C} : $[-1.3, 0.2] \times [-0.5, 0.5]$ ($\text{Re} \times \text{Im}$)
- Grid in \mathbb{C} : $152 \times 101 = 15,352$ singular values (7,752 computed)
- Plotted contour lines: $\varepsilon \in \{-0.5, -1, \dots, -3.5\}$

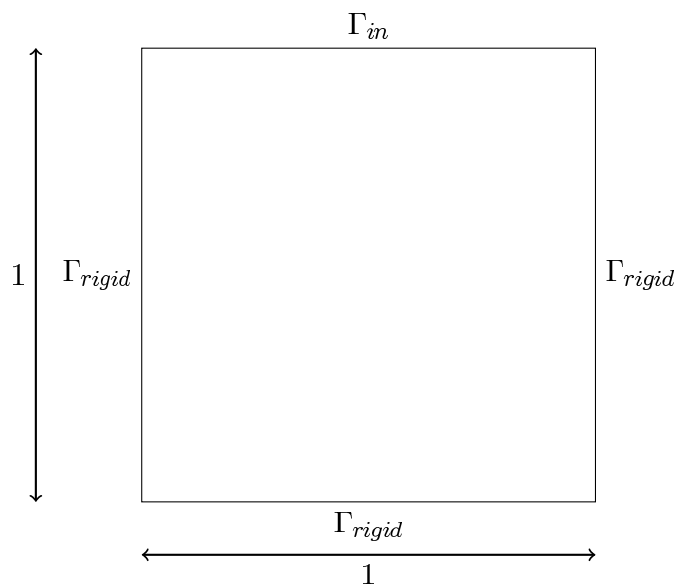


Figure 2: Geometry of the flow region.

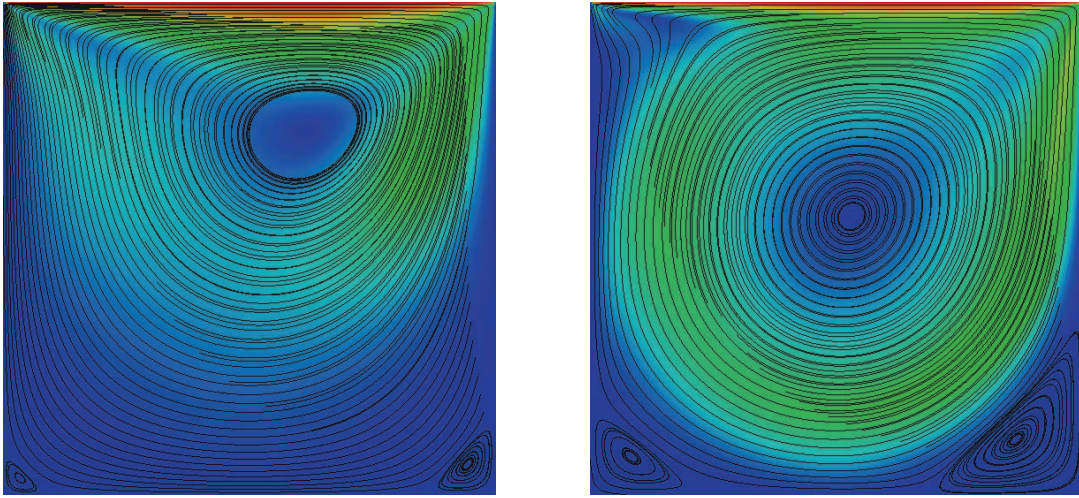
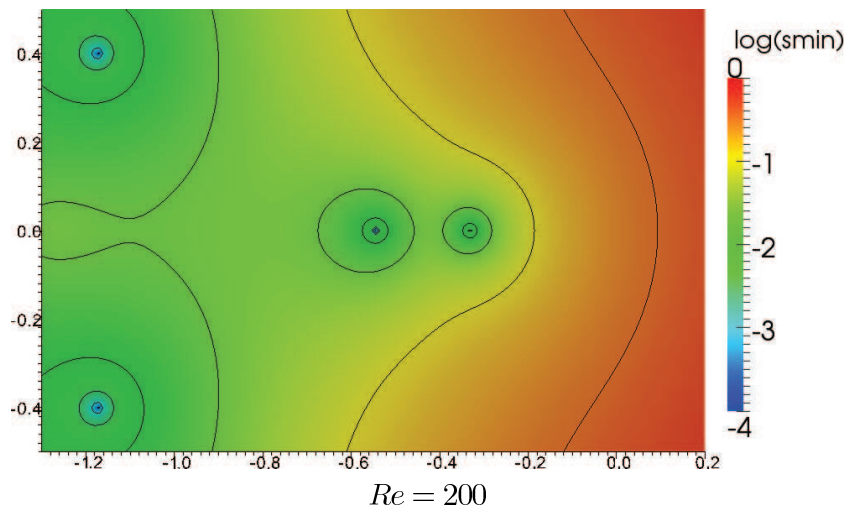
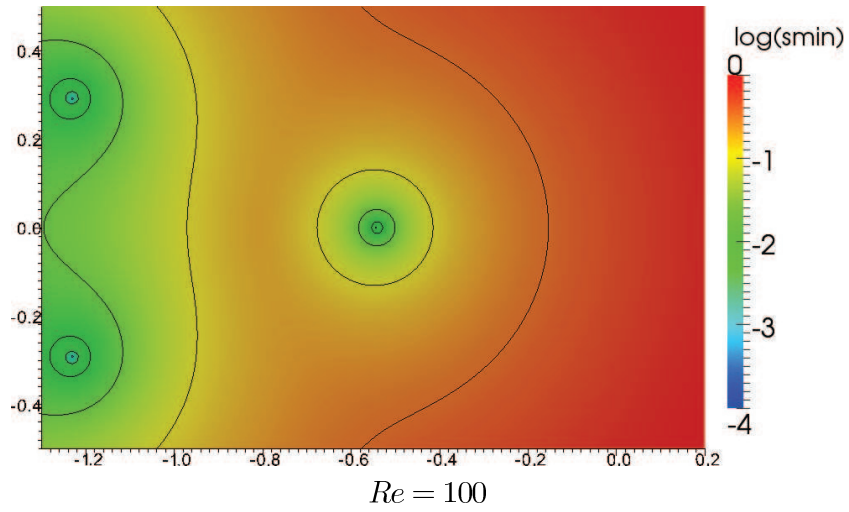
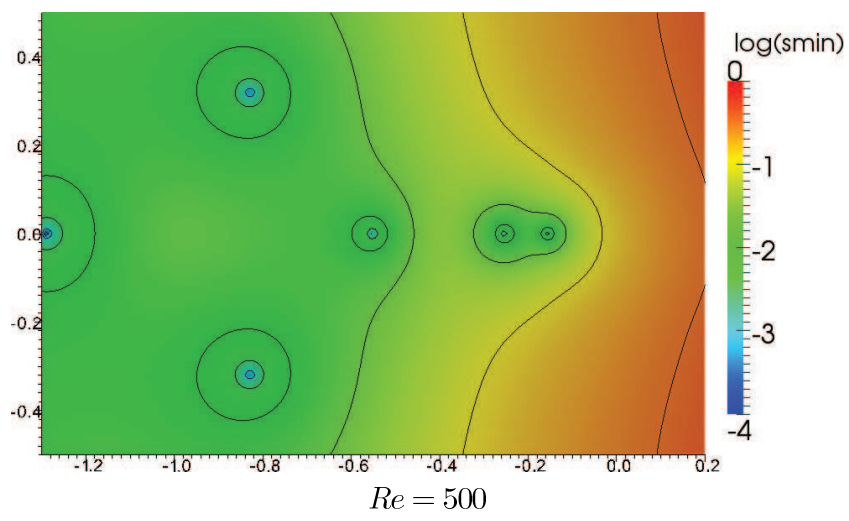
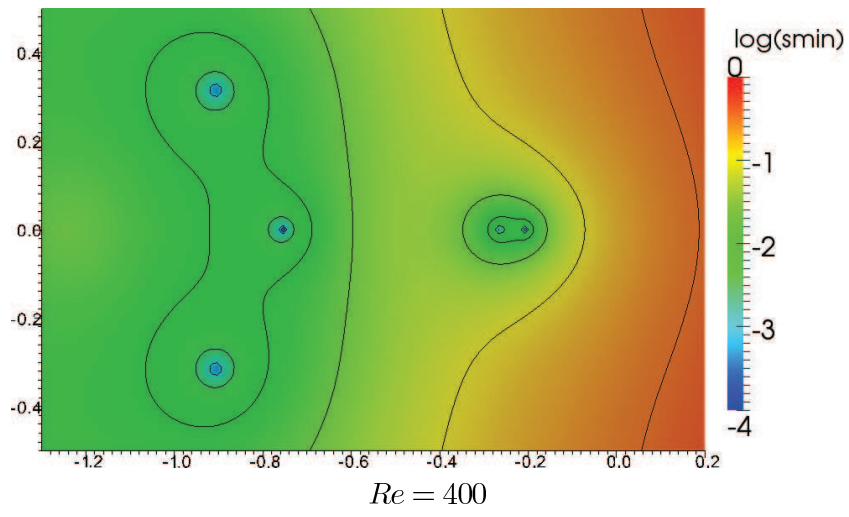
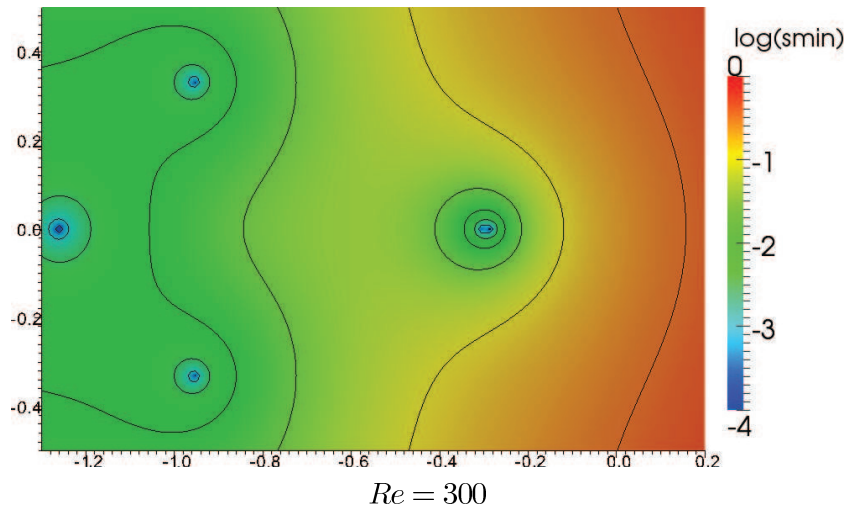
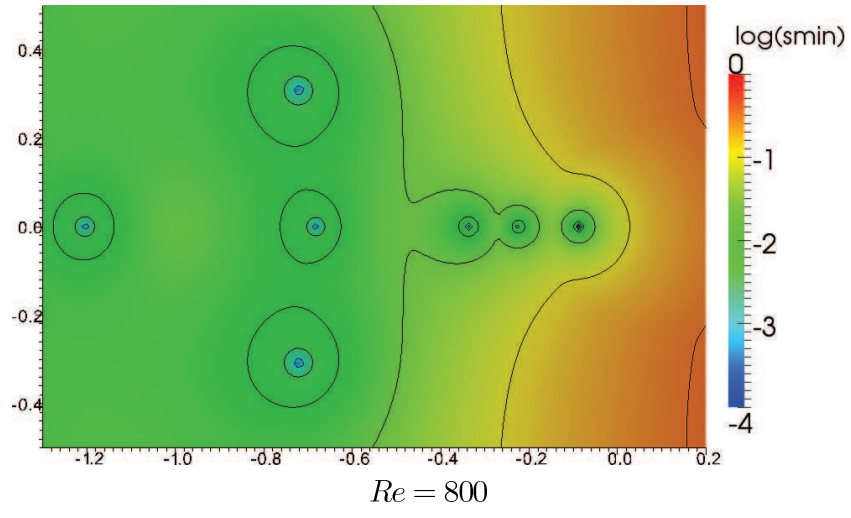
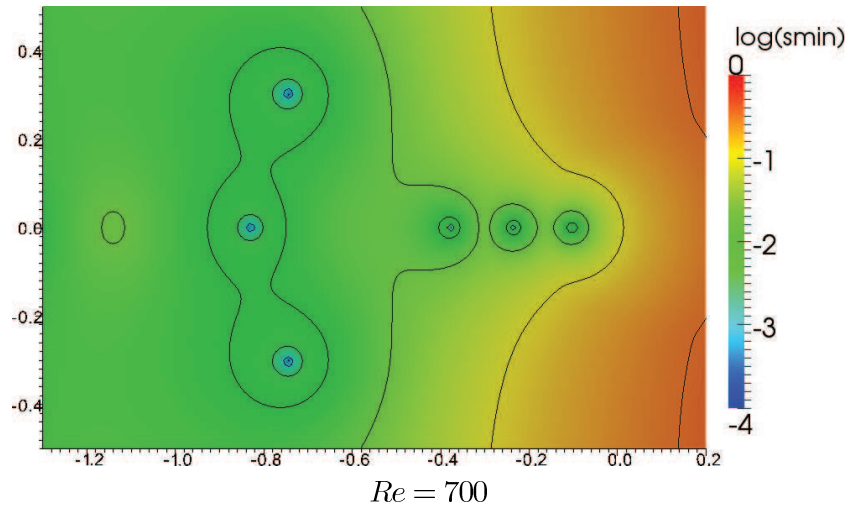
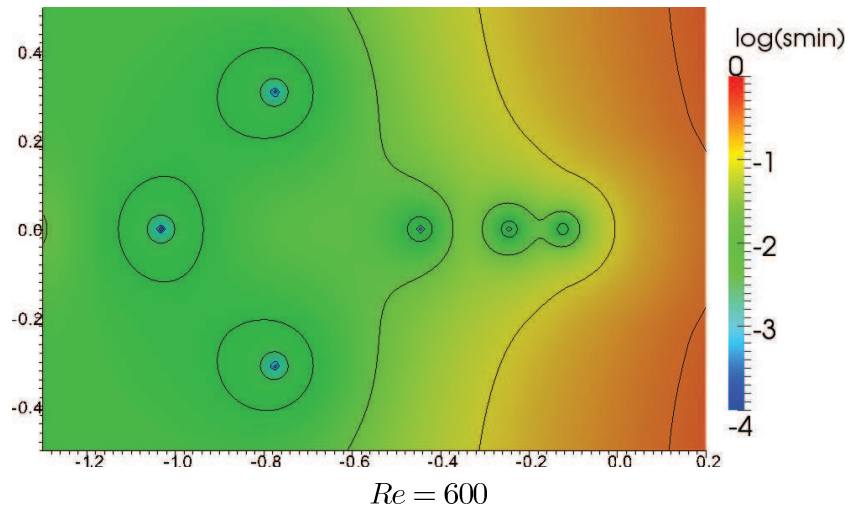
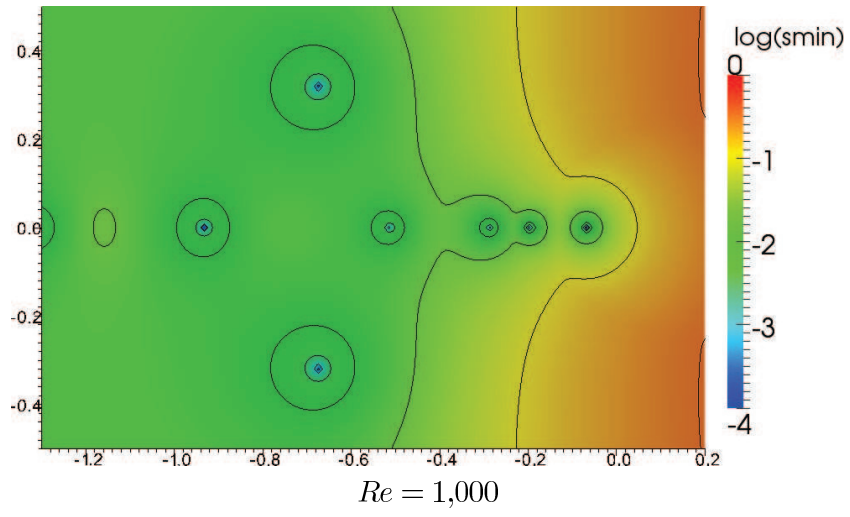
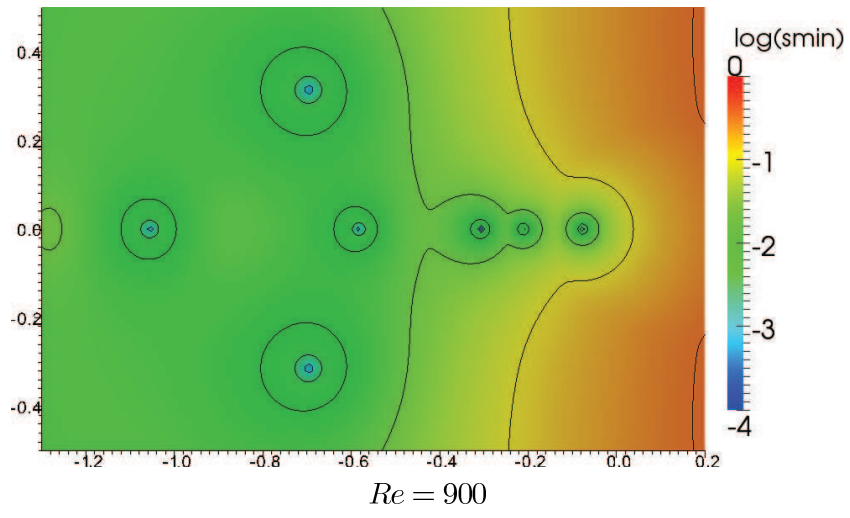


Figure 3: Steady flow of the lid-driven cavity benchmark with $Re = 100$ (left) and $Re = 1,000$ (right).









4.2 A Zig-zag Benchmark

The fluid flow considered in this benchmark is a modification of the two-dimensional Poiseuille flow. In our case we added some triangles to the pipe geometry of the Poiseuille problem, see Figure 4. We prescribe a parabolic inflow condition \mathbf{v}_{in} with peak velocity $V_{max} = V$.

- $n = 241,059$
- Region in \mathbb{C} : $[-2.2, 0.2] \times [-1.2, 1.2]$ (Re \times Im)
- Grid in \mathbb{C} : $152 \times 121 = 15,488$ singular values (7,808 computed)
- Plotted contour lines: $\varepsilon \in \{-1, -2, \dots, -6\}$

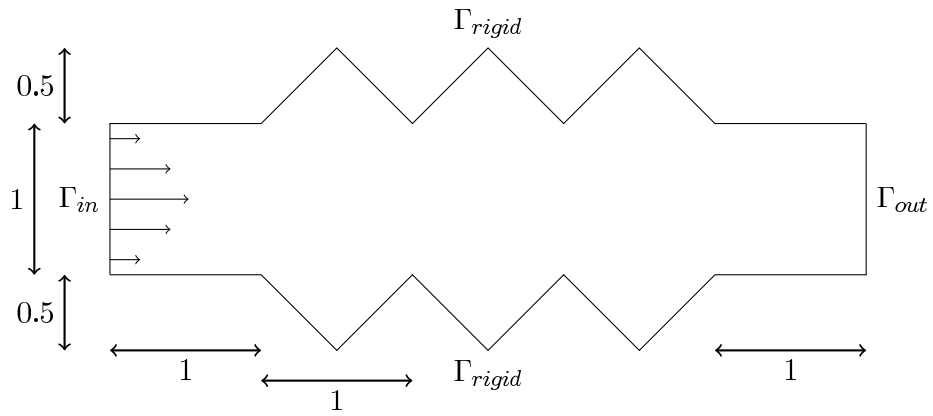
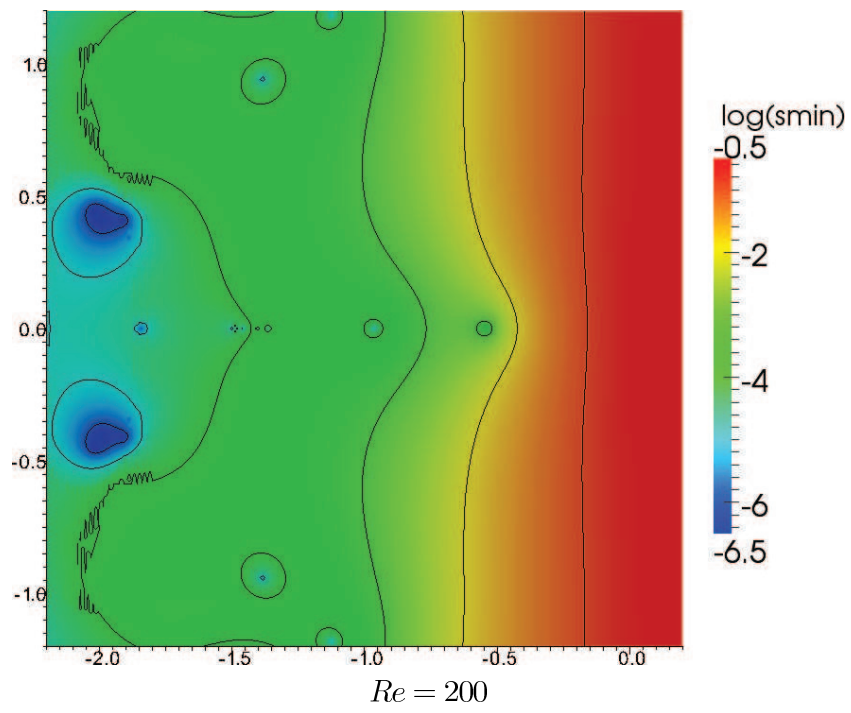
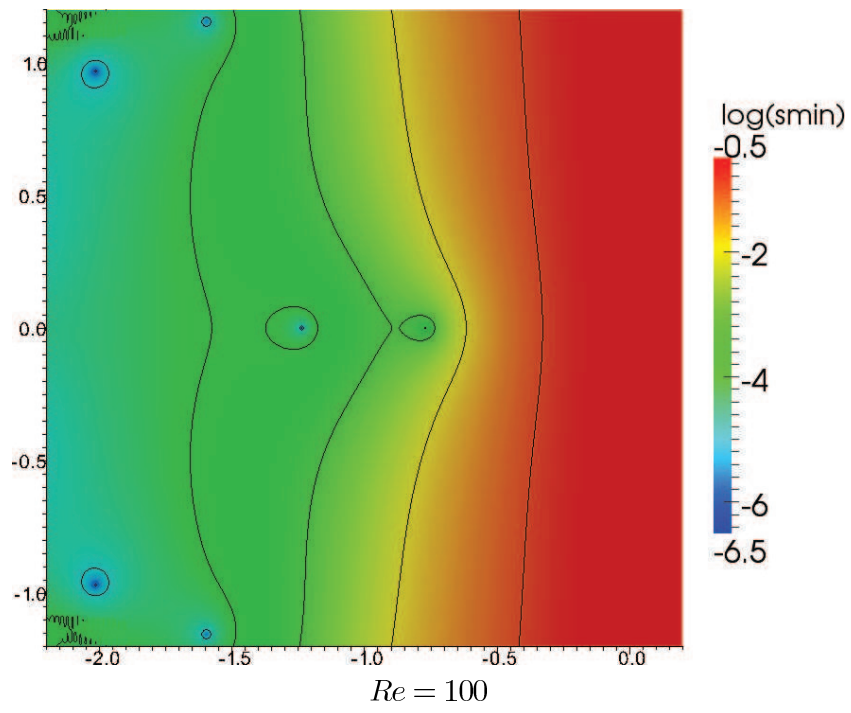
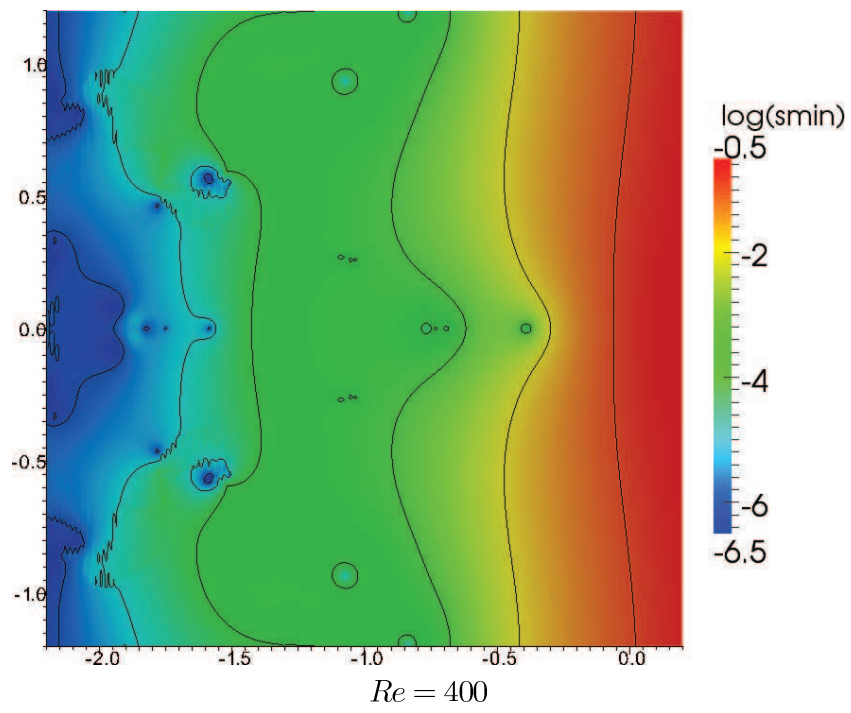
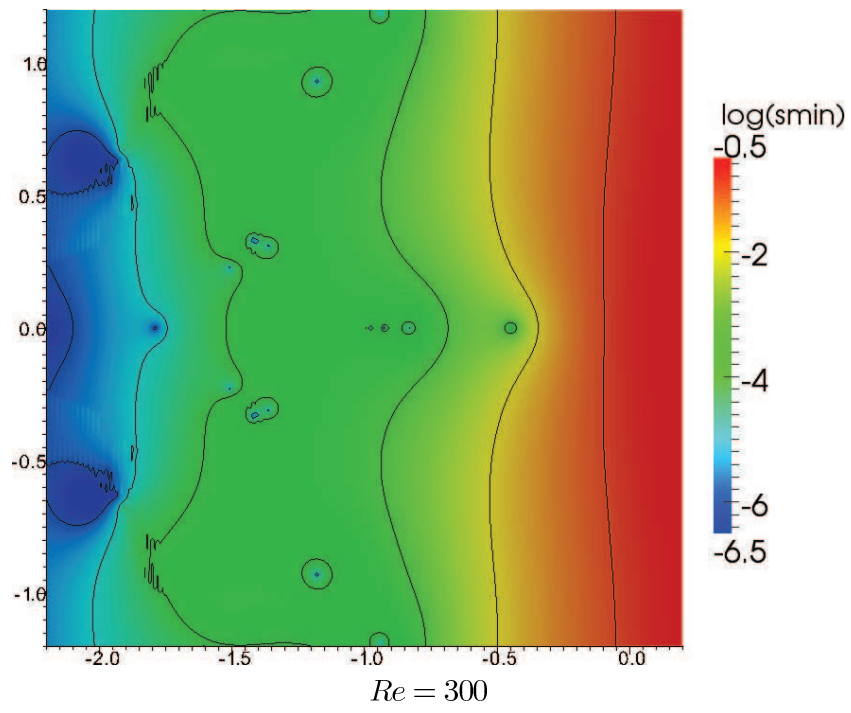


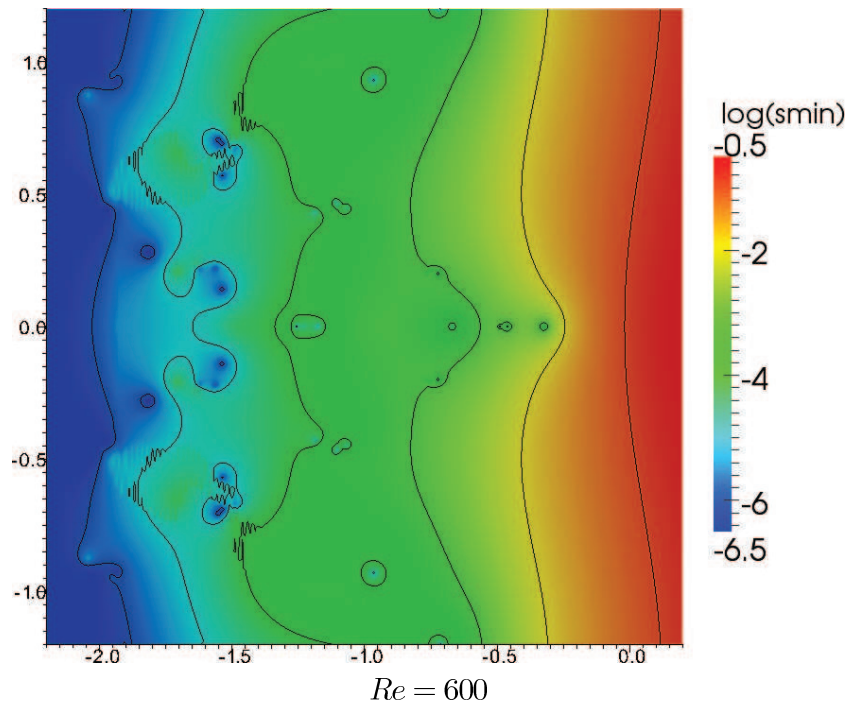
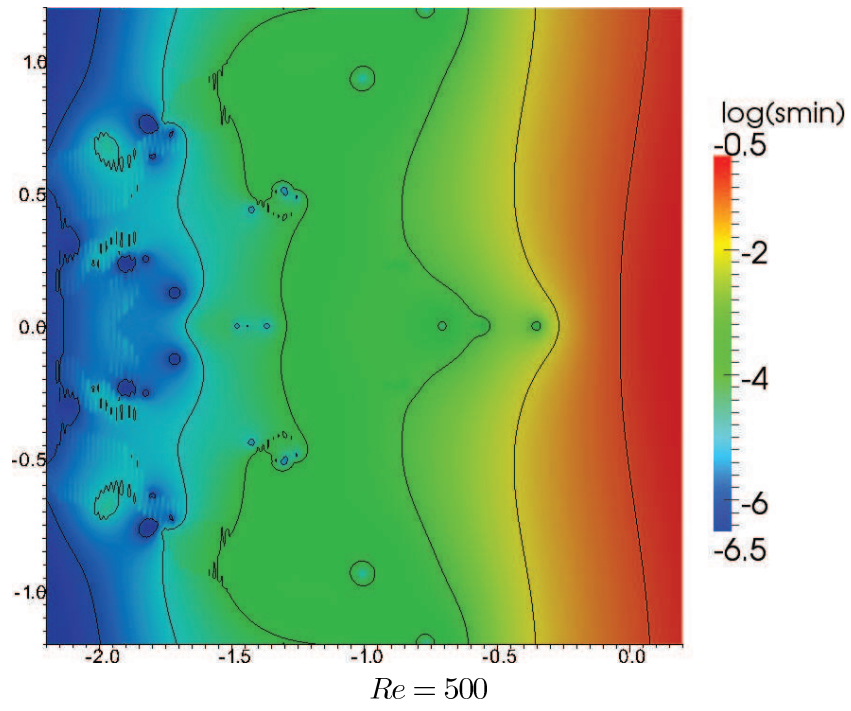
Figure 4: Geometry of the flow region.

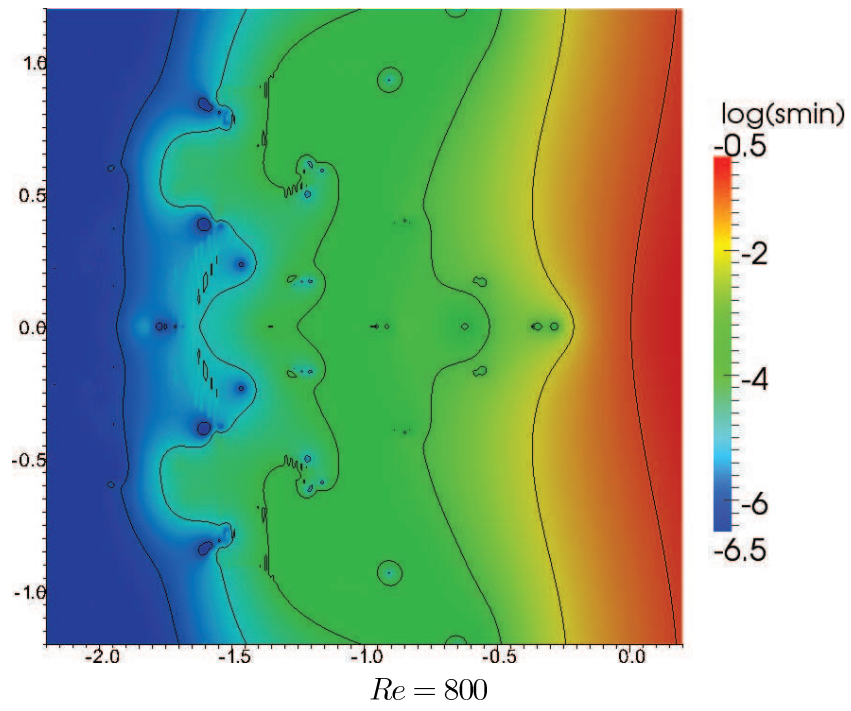
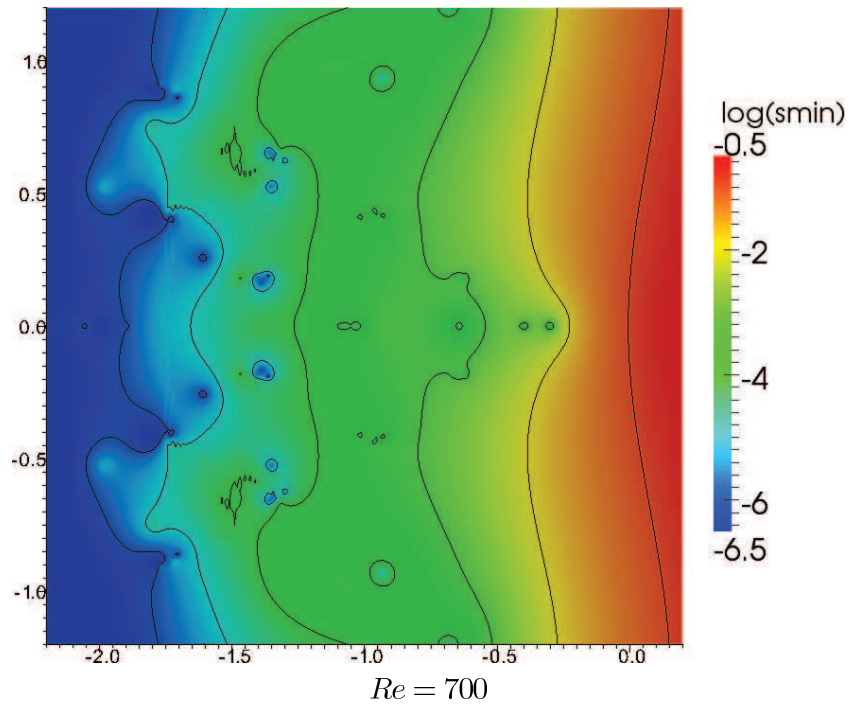


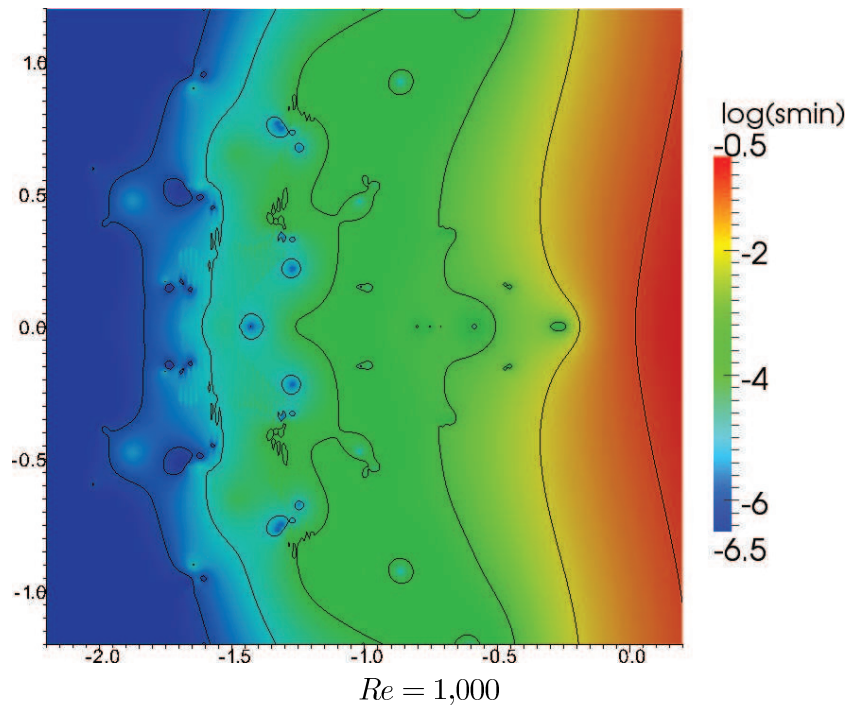
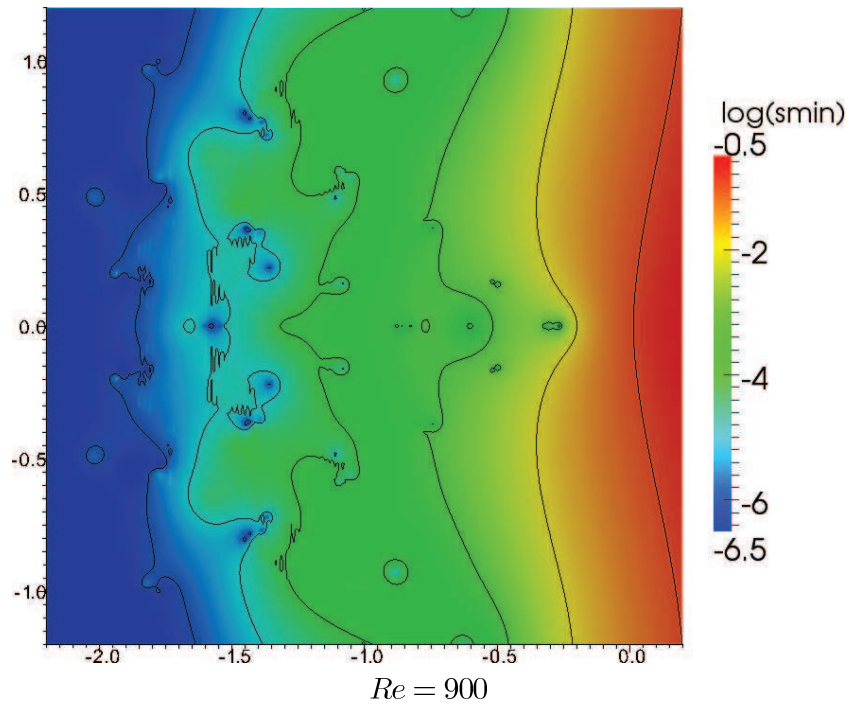
Figure 5: Steady flow in the zig-zag geometry with $Re = 100$ (upper), $Re = 500$ (middle), and $Re = 1,000$ (lower).











4.3 Flow over a Backward Facing Step

We consider a steady fluid flow over a backward facing step as depicted in Figure 6. This setup is originated from a well-known optimization problem where the vortex behind the step is to be reduced, see e.g. [6]. Here, \mathbf{v}_{in} is a parabolic inflow with peak velocity $V_{max} = V$.

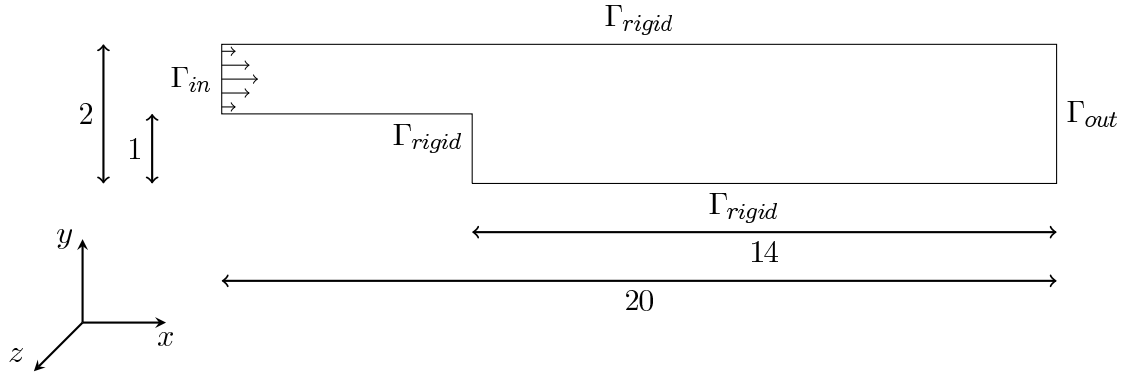


Figure 6: Geometry of the backward facing step benchmark.

4.3.1 The Two-dimensional Case

- $n = 259,971$
- Region in \mathbb{C} : $[-0.6, 0.2] \times [-0.5, 0.5]$ (Re \times Im)
- Grid in \mathbb{C} : $88 \times 101 = 8,888$ singular values (4,488 computed)
- Plotted contour lines: $\varepsilon \in \{-7, -6, \dots, -1\}$

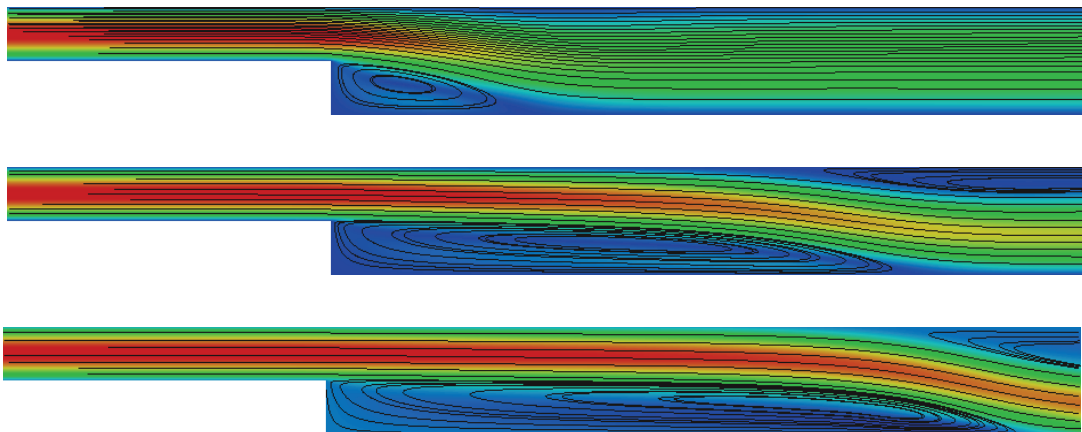
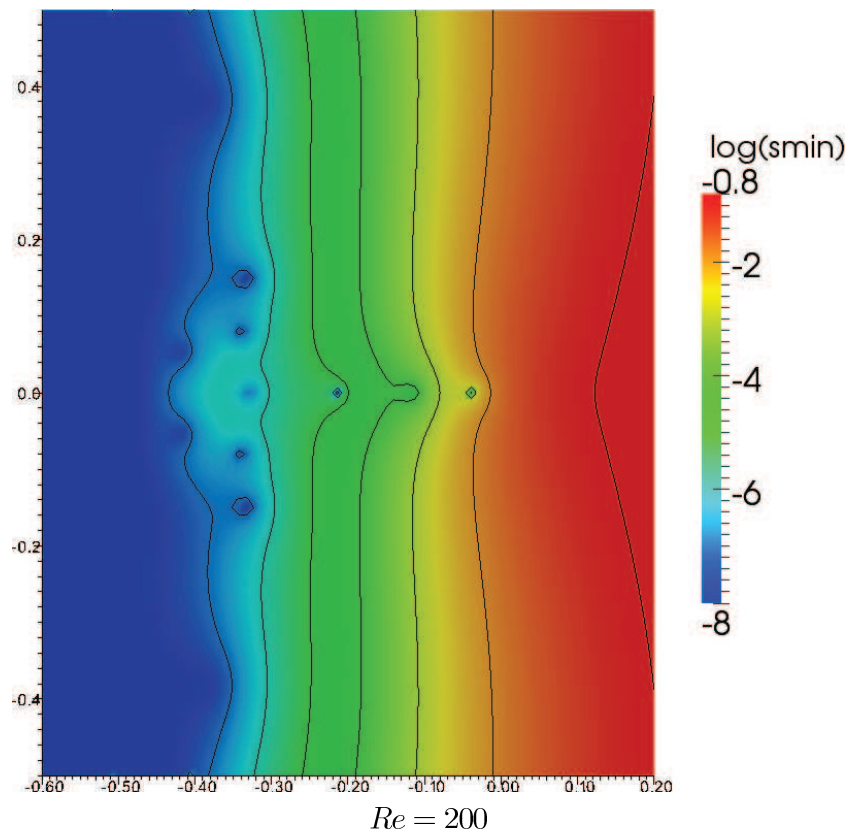
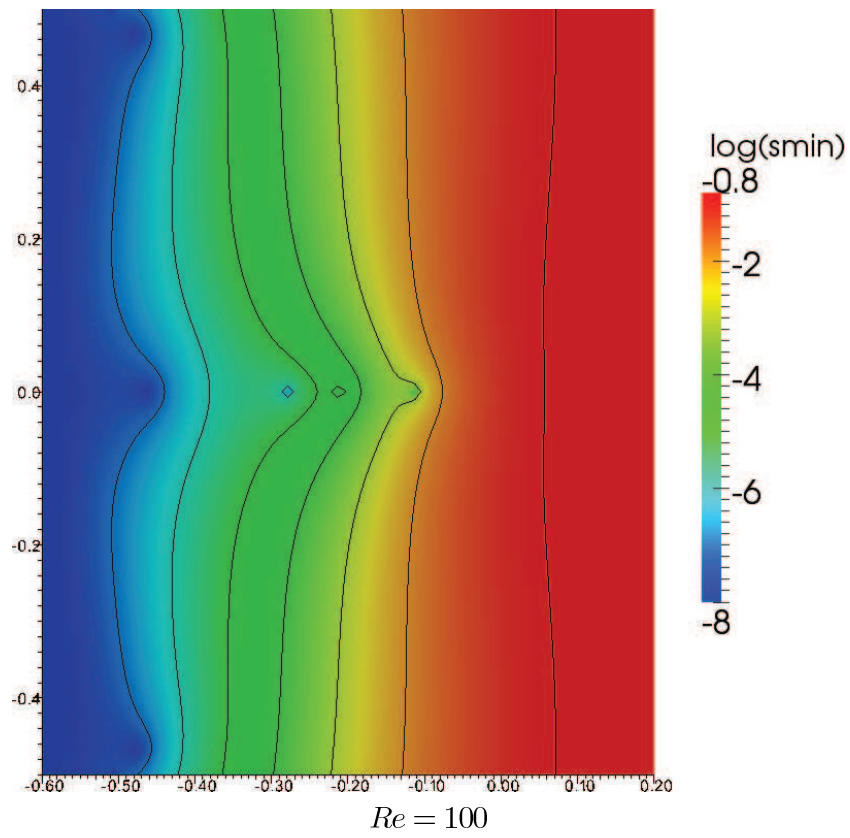
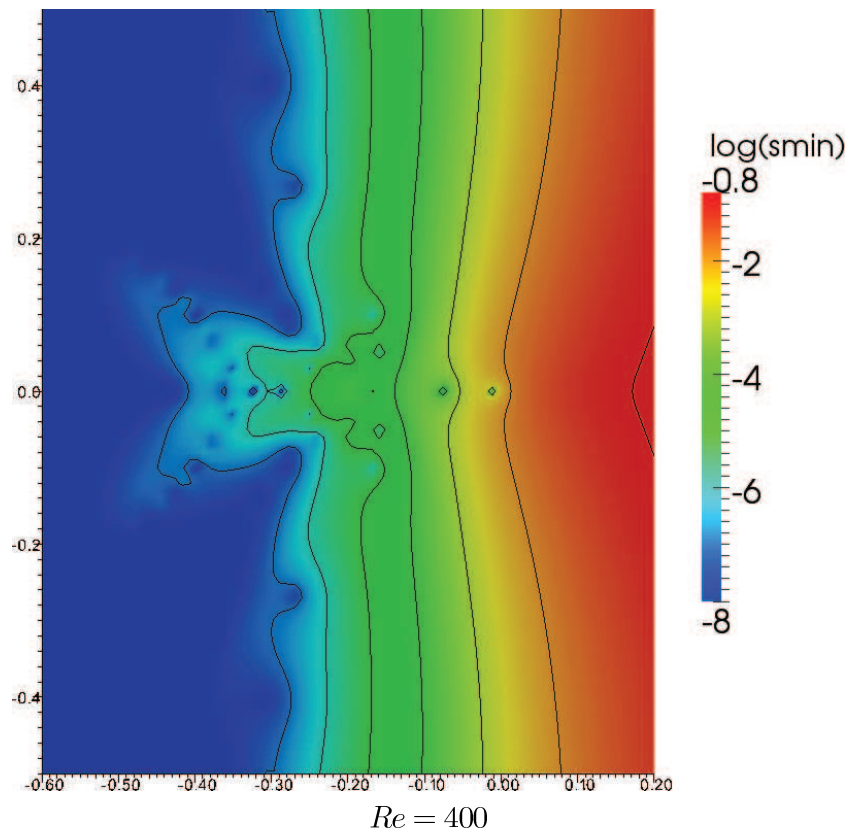
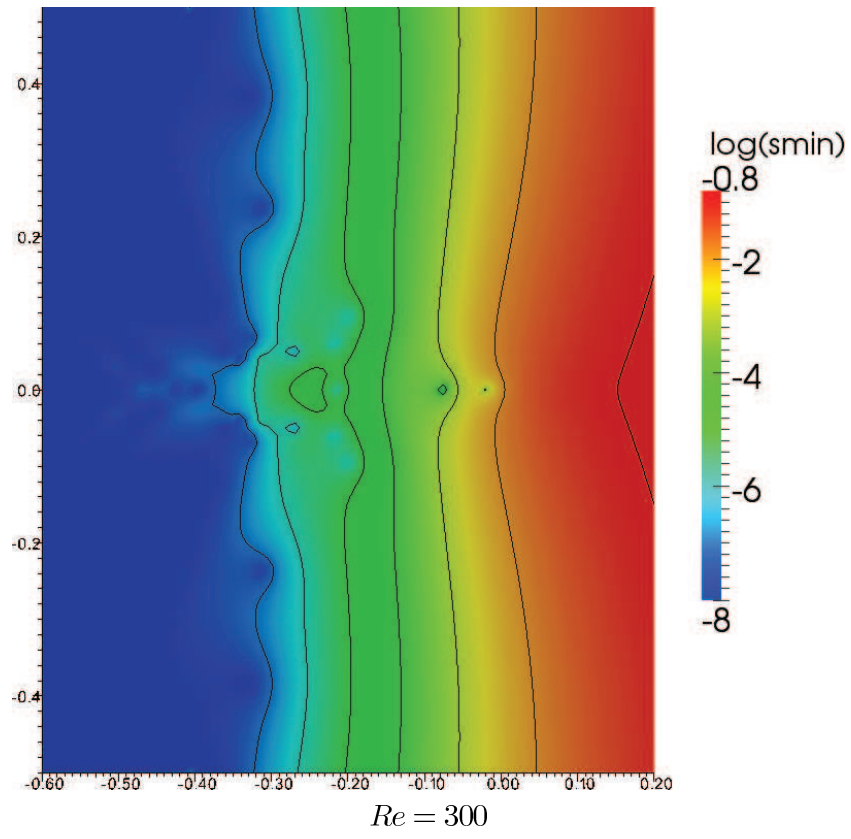
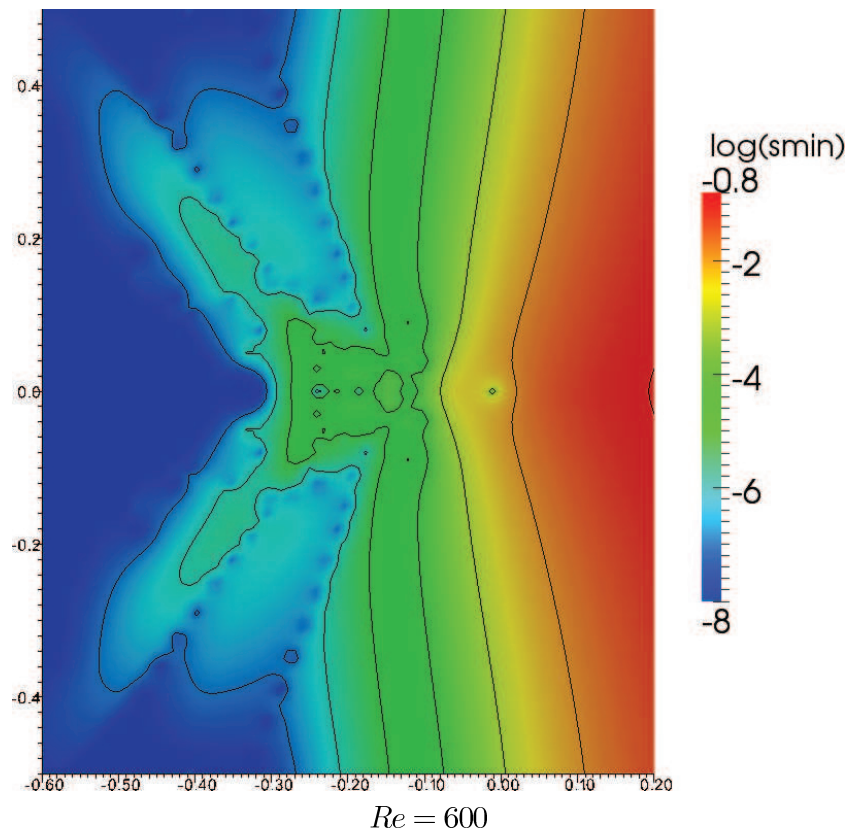
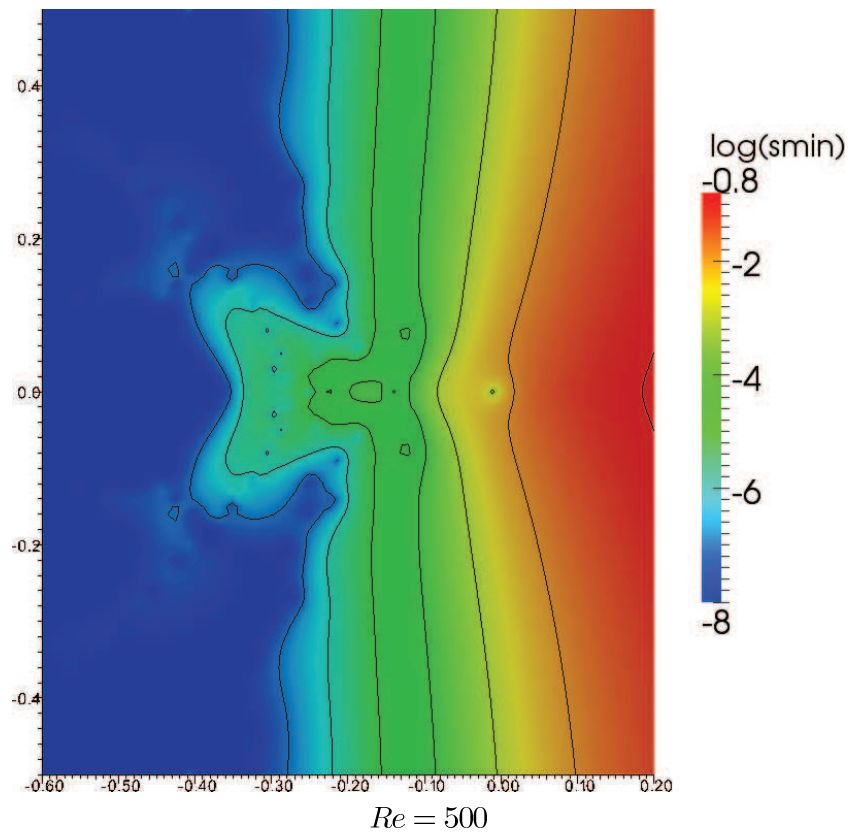
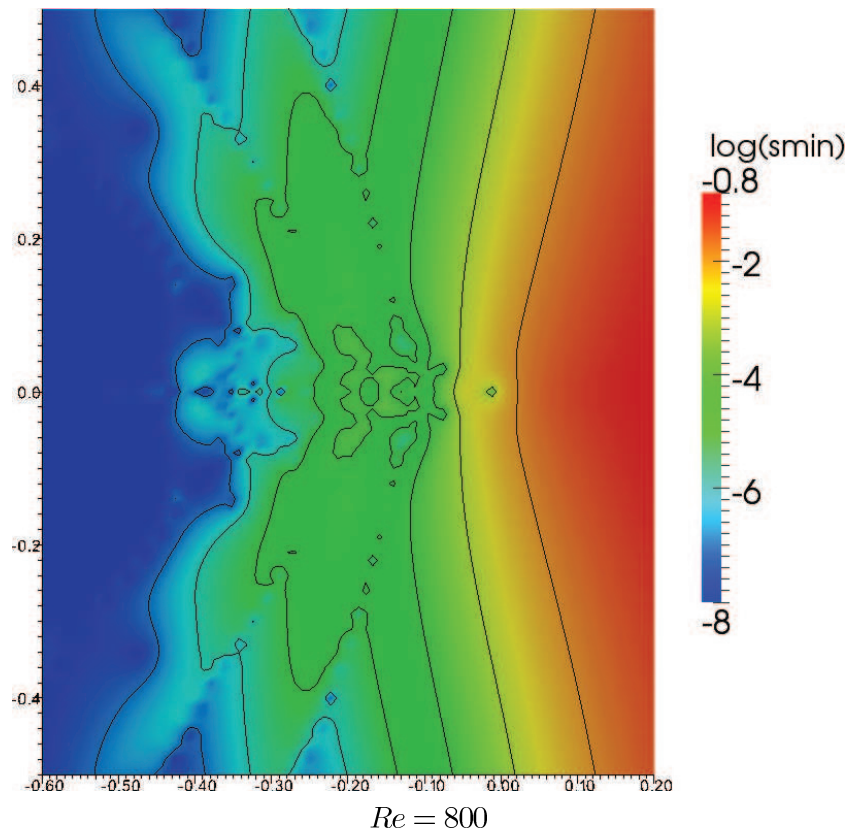
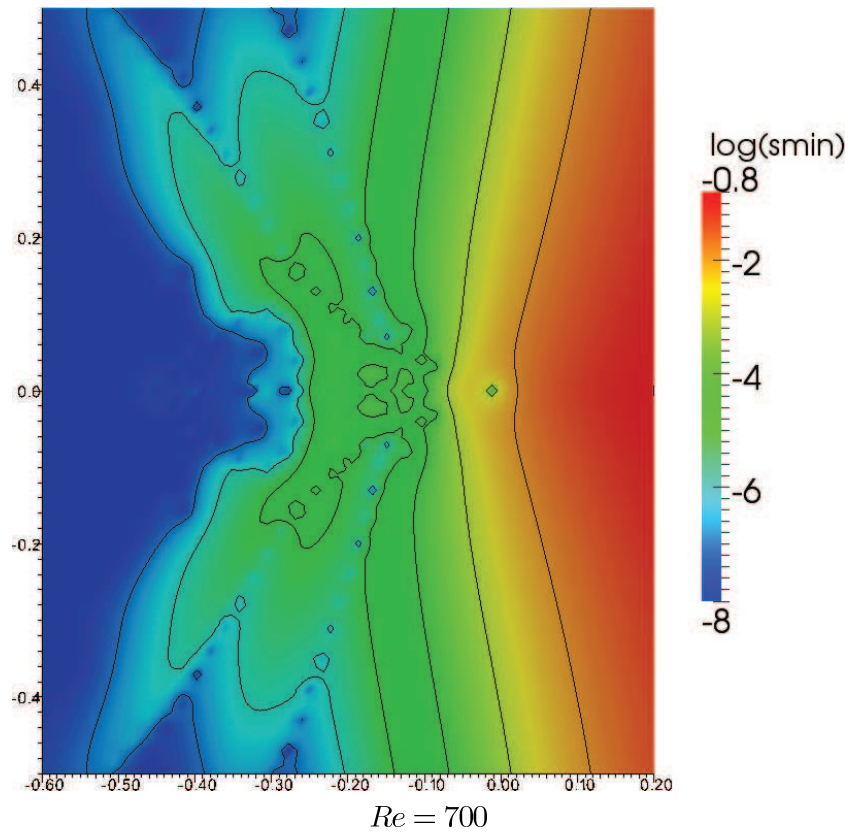


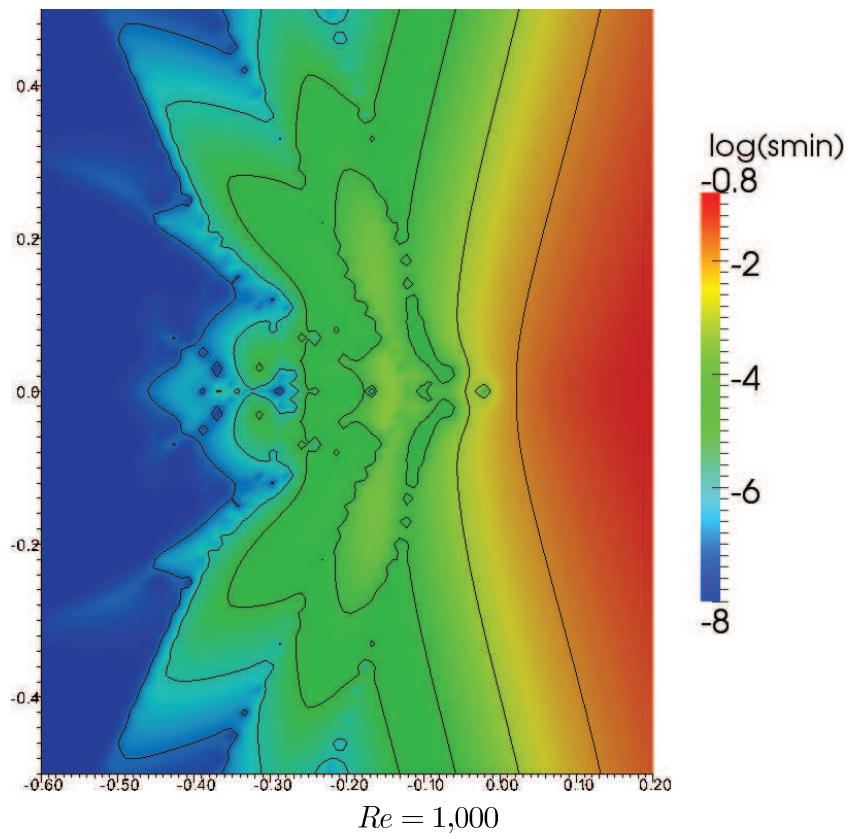
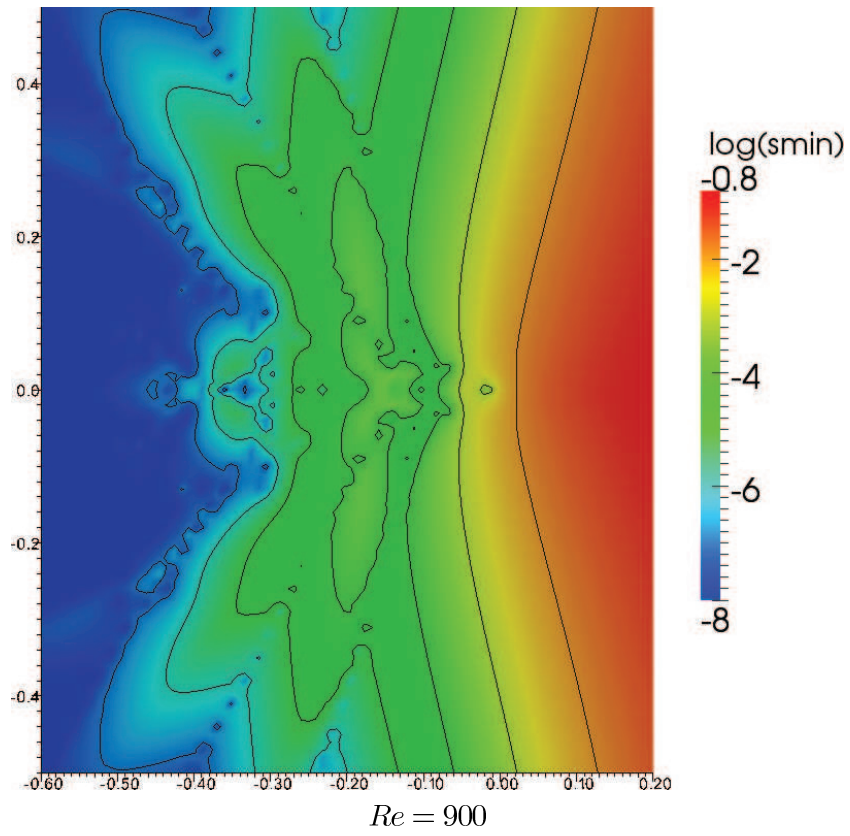
Figure 7: Stationary flow in the two-dimensional backward facing step geometry with $Re = 100$ (upper), $Re = 500$ (middle), and $Re = 1,000$ (lower).











4.3.2 The Three-dimensional Case

- $n = 143,484$
- Region in \mathbb{C} : $[-0.6, 0.2] \times [-0.5, 0.5]$ ($\text{Re} \times \text{Im}$)
- Grid in \mathbb{C} : $88 \times 101 = 8,888$ singular values (4,488 computed)
- Plotted contour lines: $\varepsilon \in \{-7, -6, \dots, -1\}$

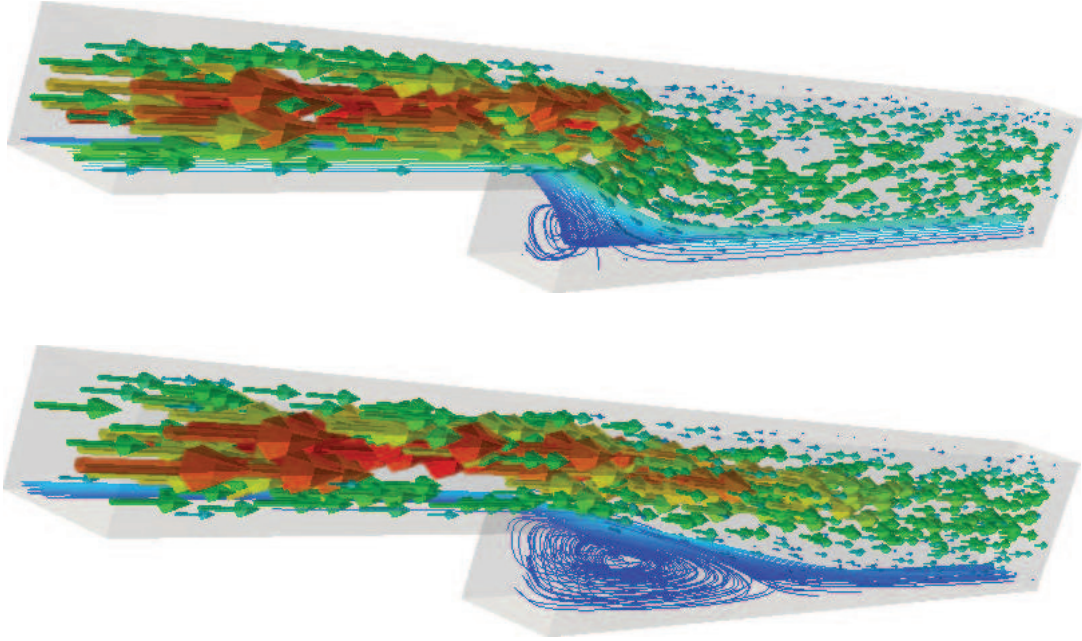
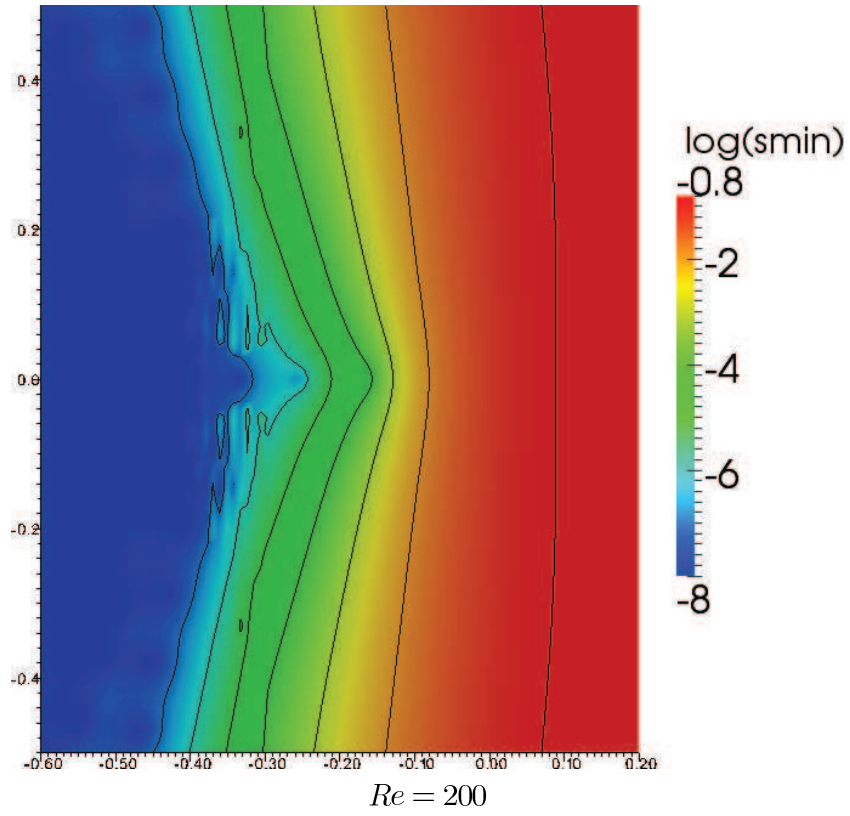
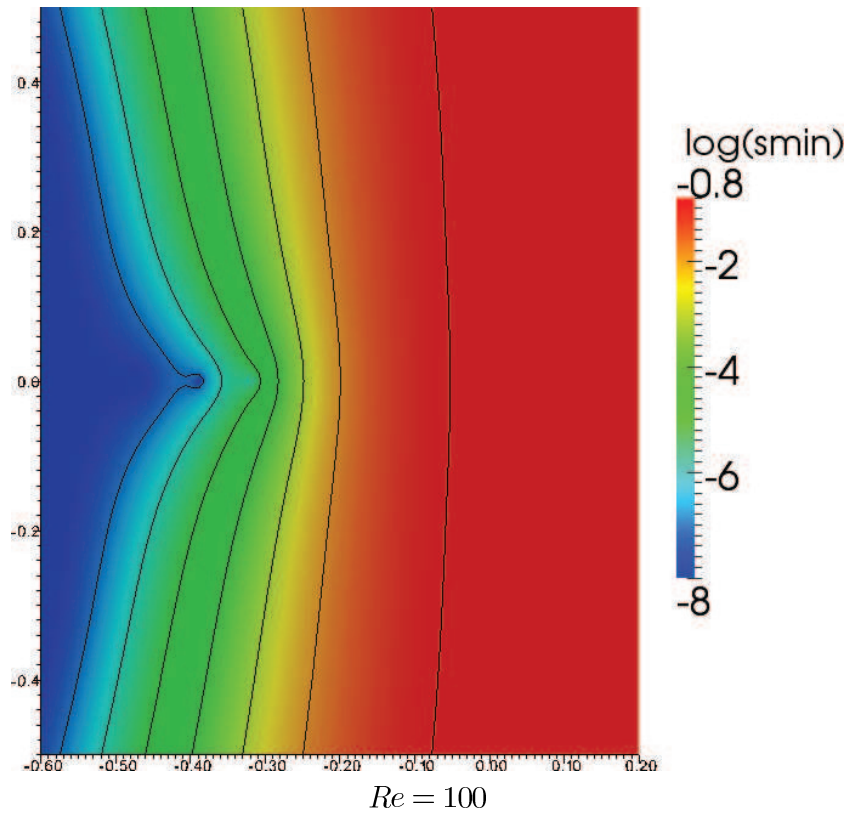
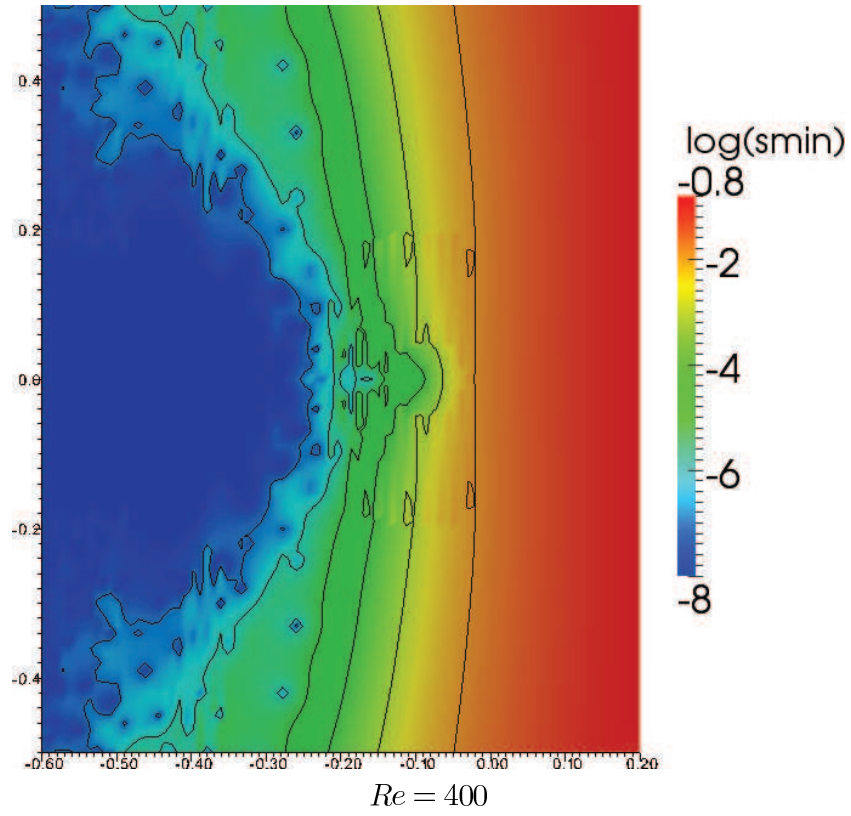
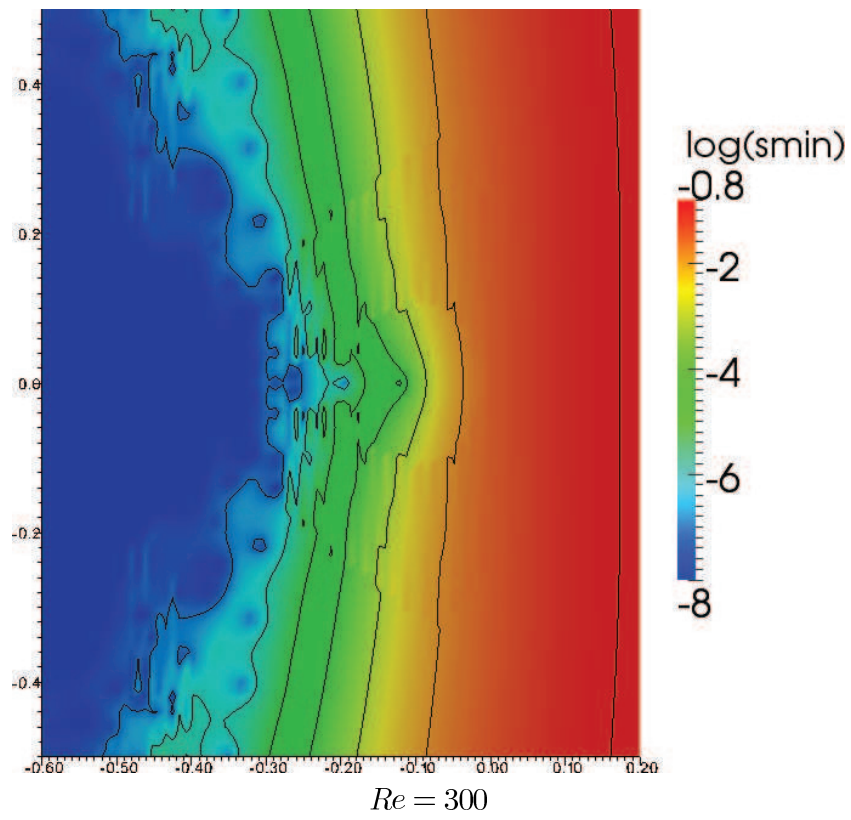
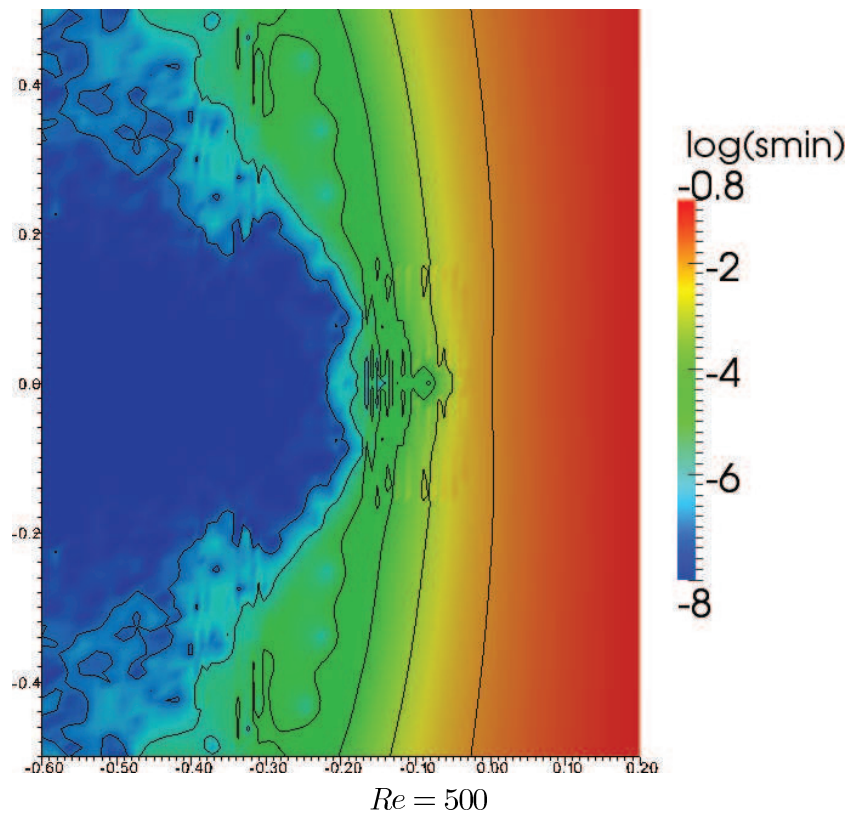


Figure 8: Stationary flow in the three-dimensional backward facing step geometry with $Re = 100$ (upper) and $Re = 500$ (lower).







References

- [1] ANZT, H., AUGUSTIN, W., BAUMANN, M., BOCKELMANN, H., GENGENBACH, T., HAHN, T., HEUVELINE, V., KETELAER, E., LUKARSKI, D., OTZEN, A., RITTERBUSCH, S., ROCKER, B., RONNÅS, S., SCHICK, M., SUBRAMANIAN, C., WEISS, J.-P., AND WILHELM, F. HiFlow³ - a flexible and hardware-aware parallel finite element package. EMCL Preprint Series, 2010.
- [2] BABUSKA, I., AND OSBORN, J. Eigenvalue problems. In *Finite Element Methods (Part 1)*, vol. 2 of *Handbook of Numerical Analysis*. Elsevier, 1991, pp. 641–787.
- [3] BOZEMAN, J. D., AND DALTON, C. Numerical study of viscous flow in a cavity. *Journal of Computational Physics* 12, 3 (1973), 348–363.
- [4] BRAMBLE, J. H., AND OSBORN, J. E. Rate of convergence estimates for non-selfadjoint eigenvalue approximations. *Mathematics of Computation* 27, 123 (1973), 525–549.
- [5] CARPRAUX, J. F., ERHEL, J., AND SADKANE, M. Spectral portrait for non hermitian large sparse matrices. *Computing* 53 (1994), 301–310.
- [6] CHOI, H., HINZE, M., AND KUNISCH, K. Instantaneous control of backward-facing step flows. *Applied Numerical Mathematics* 31, 2 (1999), 133–158.
- [7] CROUZEIX, M., PHILIPPE, B., AND SADKANE, M. The Davidson method. *SIAM Journal on Scientific Computing* 15 (1994), 62–76.
- [8] DAVIDSON, E. R. The iterative calculation of a few of the lowest eigenvalues and corresponding eigenvectors of large real-symmetric matrices. *Journal of Computational Physics* 17 (1975), 87–94.
- [9] DRAZIN, P. G. *Introduction to hydrodynamic stability*. Cambridge texts in applied mathematics ; 32. Cambridge University Press, 2002.
- [10] DRAZIN, P. G., AND REID, W. H. *Hydrodynamic Stability*, 2nd ed. Cambridge University Press, 2004.
- [11] HEUVELINE, V., PHILIPPE, B., AND SADKANE, M. Parallel computation of spectral portrait of large matrices by Davidson type methods. *Numerical Algorithms* 16, 1 (1997), 55–75.
- [12] HEUVELINE, V., SUBRAMANIAN, C., LUKARSKI, D., AND WEISS, J.-P. A multi-platform linear algebra toolbox for finite element solvers on heterogeneous clusters. In *IEEE Cluster 2010, Workshop on Parallel Programming and Applications on Accelerator Clusters (PPAAC 2010)* (Heraklion, Greece, September 20–24, 2010).
- [13] OSBORN, J. E. Spectral approximation for compact operators. *Mathematics of Computation* 29, 131 (1975), 712–725.
- [14] OSBORN, J. E. Approximation of the eigenvalues of a nonselfadjoint operator arising in the study of the stability of stationary solutions of the Navier-Stokes equations. *SIAM Journal on Numerical Analysis* 13, 2 (1976), 185–197.

- [15] PHILIPPE, B., AND SADKANE, M. Computation of the fundamental singular subspace of a large matrix. *Linear Algebra and its Applications* 257 (1997), 77–104.
- [16] SUBRAMANIAN, C. High performance computing for stability problems – Applications to hydrodynamic stability and neutron transport criticality. Dissertationsschrift, Karlsruhe Institute of Technology, 2011.
- [17] TREFETHEN, L. N., AND EMBREE, M. *Spectra and pseudospectra*. Princeton University Press, 2005.
- [18] TREFETHEN, L. N., TREFETHEN, A. E., REDDY, S. C., AND DRISCOLL, T. A. Hydrodynamic stability without eigenvalues. *Science* 261, 5121 (1993), 578–584.

Preprint Series of the Engineering Mathematics and Computing Lab

recent issues

- No. 2012-02 Dominik P.J. Barz, Hendryk Bockelmann, Vincent Heuveline: Electrokinetic optimization of a micromixer for lab-on-chip applications
- No. 2012-01 Sven Janko, Björn Rocker, Martin Schindewolf, Vincent Heuveline, Wolfgang Karl: Software Transactional Memory, OpenMP and Pthread implementations of the Conjugate Gradients Method - a Preliminary Evaluation
- No. 2011-17 Hartwig Anzt, Jack Dongarra, Vincent Heuveline, Piotr Luszczek: GPU-Accelerated Asynchronous Error Correction for Mixed Precision Iterative Refinement
- No. 2011-16 Vincent Heuveline, Sebastian Ritterbusch, Staffan Ronnås: Augmented Reality for Urban Simulation Visualization
- No. 2011-15 Hartwig Anzt, Jack Dongarra, Mark Gates, Stanimire Tomov: Block-asynchronous multigrid smoothers for GPU-accelerated systems
- No. 2011-14 Hartwig Anzt, Jack Dongarra, Vincent Heuveline, Stanimire Tomov: A Block-Asynchronous Relaxation Method for Graphics Processing Units
- No. 2011-13 Vincent Heuveline, Wolfgang Karl, Fabian Nowak, Mareike Schmidtobreck, Florian Wilhelm: Employing a High-Level Language for Porting Numerical Applications to Reconfigurable Hardware
- No. 2011-12 Vincent Heuveline, Gudrun Thäter: Proceedings of the 4th EMCL-Workshop Numerical Simulation, Optimization and High Performance Computing
- No. 2011-11 Thomas Gengenbach, Vincent Heuveline, Mathias J. Krause: Numerical Simulation of the Human Lung: A Two-scale Approach
- No. 2011-10 Vincent Heuveline, Dimitar Lukarski, Fabian Oboril, Mehdi B. Tahoori, Jan-Philipp Weiss: Numerical Defect Correction as an Algorithm-Based Fault Tolerance Technique for Iterative Solvers
- No. 2011-09 Vincent Heuveline, Dimitar Lukarski, Nico Trost, Jan-Philipp Weiss: Parallel Smoothers for Matrix-based Multigrid Methods on Unstructured Meshes Using Multicore CPUs and GPUs
- No. 2011-08 Vincent Heuveline, Dimitar Lukarski, Jan-Philipp Weiss: Enhanced Parallel $ILU(p)$ -based Preconditioners for Multi-core CPUs and GPUs – The $Power(q)$ -pattern Method
- No. 2011-07 Thomas Gengenbach, Vincent Heuveline, Rolf Mayer, Mathias J. Krause, Simon Zimny: A Preprocessing Approach for Innovative Patient-specific Intranasal Flow Simulations
- No. 2011-06 Hartwig Anzt, Maribel Castillo, Juan C. Fernández, Vincent Heuveline, Francisco D. Igual, Rafael Mayo, Enrique S. Quintana-Ortí: Optimization of Power Consumption in the Iterative Solution of Sparse Linear Systems on Graphics Processors
- No. 2011-05 Hartwig Anzt, Maribel Castillo, José I. Aliaga, Juan C. Fernández, Vincent Heuveline, Rafael Mayo, Enrique S. Quintana-Ortí: Analysis and Optimization of Power Consumption in the Iterative Solution of Sparse Linear Systems on Multi-core and Many-core Platforms